REPORT DOCUMENTATION PAGE

Form Approved
OMB No. 0704-0188

1. AGENCY USE ONLY (Leave blank)	2. REPORT DATE	3. REPORT TYPE AND DATES COVERED
	6/25/96	Annual Report 07/01/95-06/30/96

4. TITLE AND SUBTITLE

Experimental Studies of Electro-Mechanical Transduction in Thin-Film Polyurethane

5. FUNDING NUMBERS

G

6. AUTHOR(S)

Qiming Zhang

7. PERFORMING ORGANIZATION NAME(S) AND ADDRESS(ES)

Materials Research Laboratory
The Penn State University
University Park, PA 16802

8. PERFORMING ORGANIZATION REPORT NUMBER

9. SPONSORING/MONITORING AGENCY NAME(S) AND ADDRESS(ES)

Wallace A. Smith
ONR 332
Office of Naval Research
Ballston Tower One
800 No. Quincy St., Arlington

Office of Naval Research
Regional Office Chicago
536 S. Clark Street, Room 208
Chicago, IL 60605-1588

10. SPONSORING/MONITORING AGENCY REPORT NUMBER

11. SUPPLEMENTARY NOTES

12a. DISTRIBUTION/AVAILABILITY STATEMENT

distribution is unlimited

13. ABSTRACT *(Maximum 200 words)*

This report describes the results of an experimental investigation on the electromechanical response of a polyurethane elastomer (Dow 2103-80AE). The results show that the Maxwell stress contribution to the strain response can be significant at temperatures higher than the glass transition temperature. On the other hand, the material exhibits a very high electrostrictive coefficient Q, about two orders of magnitude higher than that of PVDF. The experimental results reveal that in a polymeric material, the chain segment motions can be divided into those related to the polarization response and those related to the mechanical response and the overlap region between the two yields the electromechanical response of the material. Experimental evidence indicates that the average energy barrier for the mechanical related segment motions is higher than that of non-mechanical related segment motions. To identify the molecular origins of these segment motions, FTIR and DSC were carried out at room temperature and above. ESCA and uniform distribution of the soft segments and hard segments along the sample thickness direction and it was observed that depending on the surface conditions, the ratio between the two in the surface region can be different from the bulk, which may be responsible for the enhanced electromechanical response in thin film samples. A unique apparatus is nearly completed and will make reliable and easy the measurement of the field induced strain of soft and thin polymeric materials.

14. SUBJECT TERMS	15. NUMBER OF PAGES
Transducer Materials, Electromechanical Behavior, Polyurethane	16. PRICE CODE

17. SECURITY CLASSIFICATION OF REPORT	18. SECURITY CLASSIFICATION OF THIS PAGE	19. SECURITY CLASSIFICATION OF ABSTRACT	20. LIMITATION OF ABSTRACT
Unclassified	Unclassified	Unclassified	SAR

GENERAL INSTRUCTIONS FOR COMPLETING SF 298

The Report Documentation Page (RDP) is used in announcing and cataloging reports. It is important that this information be consistent with the rest of the report, particularly the cover and title page. Instructions for filling in each block of the form follow. It is important to ***stay within the lines*** to meet ***optical scanning requirements***.

Block 1. Agency Use Only *(Leave blank)*.

Block 2. Report Date. Full publication date including day, month, and year, if available (e.g. 1 Jan 88). Must cite at least the year.

Block 3. Type of Report and Dates Covered. State whether report is interim, final, etc. If applicable, enter inclusive report dates (e.g. 10 Jun 87 - 30 Jun 88).

Block 4. Title and Subtitle. A title is taken from the part of the report that provides the most meaningful and complete information. When a report is prepared in more than one volume, repeat the primary title, add volume number, and include subtitle for the specific volume. On classified documents enter the title classification in parentheses.

Block 5. Funding Numbers. To include contract and grant numbers; may include program element number(s), project number(s), task number(s), and work unit number(s). Use the following labels:

C	- Contract	**PR**	- Project
G	- Grant	**TA**	- Task
PE	- Program Element	**WU**	- Work Unit Accession No.

Block 6. Author(s). Name(s) of person(s) responsible for writing the report, performing the research, or credited with the content of the report. If editor or compiler, this should follow the name(s).

Block 7. Performing Organization Name(s) and Address(es). Self-explanatory.

Block 8. Performing Organization Report Number. Enter the unique alphanumeric report number(s) assigned by the organization performing the report.

Block 9. Sponsoring/Monitoring Agency Name(s) and Address(es). Self-explanatory.

Block 10. Sponsoring/Monitoring Agency Report Number. *(If known)*

Block 11. Supplementary Notes. Enter information not included elsewhere such as: Prepared in cooperation with.... Trans. of.... To be published in.... When a report is revised, include a statement whether the new report supersedes or supplements the older report.

Block 12a. Distribution/Availability Statement. Denotes public availability or limitations. Cite any availability to the public. Enter additional limitations or special markings in all capitals (e.g. NOFORN, REL, ITAR).

- **DOD** - See DoDD 5230.24, "Distribution Statements on Technical Documents."
- **DOE** - See authorities.
- **NASA** - See Handbook NHB 2200.2.
- **NTIS** - Leave blank.

Block 12b. Distribution Code.

- **DOD** - Leave blank.
- **DOE** - Enter DOE distribution categories from the Standard Distribution for Unclassified Scientific and Technical Reports.
- **NASA** - Leave blank.
- **NTIS** - Leave blank.

Block 13. Abstract. Include a brief *(Maximum 200 words)* factual summary of the most significant information contained in the report.

Block 14. Subject Terms. Keywords or phrases identifying major subjects in the report.

Block 15. Number of Pages. Enter the total number of pages.

Block 16. Price Code. Enter appropriate price code *(NTIS only)*

Blocks 17. - 19. Security Classifications. Self-explanatory. Enter U.S. Security Classification in accordance with U.S. Security Regulations (i.e., UNCLASSIFIED). If form contains classified information, stamp classification on the top and bottom of the page.

Block 20. Limitation of Abstract. This block must be completed to assign a limitation to the abstract. Enter either UL (unlimited) or SAR (same as report). An entry in this block is necessary if the abstract is to be limited. If blank, the abstract is assumed to be unlimited.

Experimental Studies of Electro-Mechanical Transduction in A Polyurethane Elastomer

Annual Report

07/01/95 - 06/30/96

Submitted to:

Wallace A. Smith
ONR 332
Office of Naval Research
Ballston Tower One
800 North Quincy Street
Arlington, VA 22217-5660

R. Ting
Naval Research Laboratory
code 251
Materials Research Division
Underwater Sound Reference Detachment
Orlando, FL 32856-8337

Submitted by:

Q.M. Zhang
Associate Professor of Materials
and Electrical Engineering
187 Materials Research Laboratory
The Pennsylvania State University
University Park, PA 16802-4800

Table of Contents

I. Introduction

Electromechanical coupling effects such as piezoelectricity and electrostriction have been widely utilized in many areas such as transducers and sensors.[1,2] Conventional electromechanical transduction materials include ceramics such as lead zirconate titanate (PZT) and lead magnesium niobate-lead titanate (PMN-PT) and single crystals such as quartz.[1,3] During the last three decades, electromechanical polymers have drawn much attention because they have high mechanical flexibility, low acoustic impedance, low manufacturing cost, and can be easily molded into desirable shapes.[4,5] However, the low electromechanical activity of the polymeric materials greatly limits their applications. For instance, the electromechanical coupling factor of the piezoelectric polyvinylidene fluoride (PVDF) and its copolymers with trifluoroethylene (TrFE), which possess the highest electromechanical activity among all the known electromechanical polymers, is less than 0.25.[6] In contrast, piezoceramic PZT has a coupling factor of 0.75.[3] Considering the fact that the energy conversion efficiency is proportional to the square of the coupling factor, the difference between the two is quite significant. Hence, there is constant searching for new polymeric materials with high electromechanical activity. Recently, it was reported that in certain polyurethane elastomers, a large electric field induced strain can be achieved and in the electric field biased state, the materials exhibit an effective piezoelectric coefficient higher than those of piezoceramic PZTs, which have stirred much excitement and interest in this class of materials.[7]

Since the discovery of this new class of materials, many experimental investigations have been conducted. It has been shown that the characteristics of the polarization response to applied electric fields indicate that the material is not a ferroelectric and the strain is proportional to the square of the applied electric field, in analogy to the electrostrictive effect.[6,7,8] Because of these features and the high elastic compliance of the material, which is in the range between 10^{-7} and 10^{-8} m^2/N, the question of whether the large electric field induced strain is caused by the Maxwell stress effect, i.e., the Coulomb interaction between the charges on the two electrodes of

the specimen, is often raised. In fact, the Coulomb attraction between the charges on the two electrodes has been widely utilized to produce actuators and transducers such as those in the current Microelectro-Mechanical Systems.[9] This possibility is reinforced by a recent experimental result which indicates that by increasing the elastic compliance of the polyurethane, the field induced strain was enhanced.[6] In addition, it was found that the electric field induced strain is very sensitive to the sample processing conditions and the thickness of the specimen.[6-8] The field induced strain by a unit electric field increases as the film thickness is reduced. It was suggested that this increase is caused by a non-uniform electric field distribution in the samples since for a strain response which is proportional to the square of the applied electric field, any non-uniform field distribution in a sample will increase the strain response. The most probable cause for this thickness dependence behavior is the existence of the surface region and the interior region, which have different electric field strength, in a specimen, and could be a result of charge injection and/or a non-uniform distribution of the material properties, as schematically drawn in figure 1(a).[6]

The objective of this investigation is to provide understanding of the possible mechanism for the observed electric field induced strain in this class of polyurethane elastomers. Through this process, we also intend to examine the nature or general features of electromechanical responses in non-ferroelectric polymeric materials. Although the dielectric and elastic responses of polymeric materials have been investigated for many decades both experimentally and theoretically and are relatively well understood,[10] the investigation on the electromechanical response in polymeric materials, except those of piezoelectricity in PVDF and its copolymers, is much less extensive and consequently, the understanding on the elastoelectric properties of polymers is relatively poor. In addition, we also intend to examine the microscopic (or mesoscopic) origin of the thickness dependent hebavior of the field induced strain (enhanced field induced strain response in thin film samples).

As has been demonstrated by many experiments, it is still a challenge to reliably measure the field induced strain on soft and thin polymeric materials. Hence, effort was devoted to the development of new techniques so that this measurement can be carried out with easy and high reliability.

II. Experimental

In this investigation, two types of experiments were conducted, one is related to examining the electromechanical response in the bulk material and the other is related to examining the possible non-uniform distribution of the soft and hard segments across the sample thickness direction which may be responsible for the observed enhanced strain response in thin film samples.

In the first part of the experiment, a relatively thick sample is used in the study. The polyurethane used is produced by Deerfield Urethane, Inc. using a Dow polyurethane (Dow 2103-80AE). In previous studies, a large field induced strain response was reported in this material.[7] The sample was cast and the thickness of the sample is 2 mm.

Polyurethane elastomer is a block copolymer with hard segments embedded in a soft segment matrix as schematically drawn in figure 1(b).[11] For the polymer investigated, the soft segment is poly(tetramethylene glycol) (PTMEG) with molecular weight of about 1000. The hard segment is comprised of a diisocyanate and a diol chain extender. The diisocyanate is methylenedi-p-phenyl diisocyanate (MDI) and the diol chain extender is 1,4-butanediol (BD). The mole ratio of the components is about

1.8 mol MDI / 0.8 mol BD / 1.0 mol PTMEG.

Hence, the hard segment (MDI + BD) is approximately 34% by weight in the sample.

The x-ray scattering result, shown in figure 2, reveals that both the hard segment and soft segment are in the amorphous phase and there is no detectable crystalline phase in the material within the experiment resolution.

In the first part of the experiments, the dielectric constant, the elastic compliance, and the electric field induced strain were characterized over a wide temperature and frequency range. In addition, FTIR and dependence of the dielectric constant on the hydrostatic pressure were also investigated over a wide temperature range.

In the second part of the experiments, ESCA and neutron surface reflectivity experiments were conducted. In the ESCA experiment, samples taken from the surface regions (with 10 micrometers of the surface regions) and from the bulk were examined and the results are compared.

The dielectric constant measurement was carried out by a HP LCR multimeter (HP 4274A), a HP impedance analyzer (HP 4192A), a capacitance bridge (General Radio 1616), and a lock-in amplifier (SR 850) depending on the capacitance value of the sample and the frequency range. The lock-in amplifier, which measures both the phase and amplitude of the voltage and current applied on the polyurethane specimen, yielding the impedance and the capacitance of the specimen, was used in the frequency range from 1 mHz to 1 kHz. The capacitance bridge covers the frequency range from 100 Hz to 100 kHz, HP LCR meter in the frequency range from 1 kHz to 1 MHz, and HP impedance analyzer in frequency from 1 kHz to 10 MHz. For the specimens with a capacitance value below 100 pF, the capacitance bridge was utilized since the error from LCR meter and impedance analyzer is quite large in measuring capacitance of small value. The temperature control was provided by a Delta chamber interfaced with a HP computer.

The electric field induced strain measurement was conducted by a double beam laser dilatometer which is equipped with a temperature chamber in the temperature range from -100 ^{o}C to about 200 ^{o}C.[12] The operating frequency range for the dilatometer is from 1 Hz to above 1 MHz. For the polymer specimens investigated, it was found that the spurious resonance existing at high frequencies made it difficult to carry out measurements to frequencies above 10 kHz.

The elastic modulus was measured by a dynamic mechanical analysis system which covers a wide frequency and temperature range.

III. Dielectric, Elastic, and Electric Field Induced Strain Responses from Bulk Polyurethane Samples:

In general, in a non-piezoelectric material such as the polyurethane elastomers investigated, the electric field induced strain can be from the electrostrictive and also from the Maxwell stress effects.[13,14] The electrostrictive effect is the direct coupling between the polarization and mechanical response in the material. It is the strain (S) or stress (T) change induced by a change in the polarization level (P) in the material which can be expressed as:

$$S = Q P^2 \qquad (1)$$

where Q is the electrostrictive coefficient of the material. For a linear dielectric where $P = \varepsilon_0 (K-1) E$, eq. (1) can be written as

$$S = Q \varepsilon_0^2 (K-1)^2 E^2 \qquad (2).$$

K is the dielectric constant of the material and ε_0 is the vacuum dielectric permittivity. On the other hand, Maxwell stress, which is due to the interaction between the free charges on the electrodes (Coulomb interaction) and to electrostatic forces that arise from dielectric inhomogeneities, can also contribute to the electric field induced strain response. For the situation considered here, it is also proportional to the square of the applied electric field (E) and it can be shown

$$T = - \varepsilon_0 K E^2 / 2 \qquad (3)$$

Hence, the dimensional change due to the Maxwell stress is

$$S = - s \varepsilon_0 K E^2 / 2 \qquad (4)$$

where s is the compliance of the material. As can be seen, for a soft material, the strain induced by the Maxwell stress can be quite substantial. In order to identify the contributions from the different mechanisms, it is necessary to measure the dielectric permittivity, the elastic compliance, and the electric field induced strain simultaneously.

For a polymeric material, it is well known that most of the material properties such as the dielectric constant and elastic compliance are very dispersive even at low frequencies, reflecting relatively high energy barriers for the motions of molecule units and chain segments.[10] Further more, the variation in the local environment and the length of the chain segments involved in the motion results in a broad distribution of the energy barriers (broad relaxation time distribution). It is also conceivable that the distribution of energy barriers for the motions of molecular units and segments which involve the strain and stress (mechanical energy) might be different from that for the motions of the segments which involves little or no strain and stress. As will be discussed later in the paper, such a difference in the energy barrier distributions between the two types of the motions will have a direct effect on the electrostrictive response of a polymeric material. Therefore, dispersion characteristics of the dielectric and elastic responses of the sample are analyzed in detail in the following.

The dielectric constant as a function of temperature is presented in figure 3. A strong frequency dispersion was observed. In the temperature range investigated, there are three relaxation peaks. The one at temperature near 20 °C is related to the glass transition which is due to the freezing process of the soft segments from a rubbery state into a glass state (α-relaxation). The one at temperatures near -100 °C is the β-relaxation which was suggested from the early studies on polyurethanes and polyamids to be related to the absorbed water molecules.[10] The nature of the relaxation at temperatures near 70 °C is unknown and is labeled as I-relaxation here. The results of a recent preliminary FTIR study suggests that it might be associated the motion in the chain extenders. Since it has no bearing on this paper, the details of that result will be presented in another publication.

The dielectric dispersion behavior was characterized over the frequency range from 0.01 Hz to 1 MHz and typical results are presented in figure 4(a). It was found that for the data at temperature range from -80 °C to 20 °C, one can make use of the temperature-frequency superposition principal to construct a master curve as illustrated in figure 4(b) for the one at 0 °C

where the data at temperatures other than 0 °C were shifted in the frequency by times a factor a(t) (a(t) * f, where f is the frequency), which is a function of temperature t.[10] For a dielectric relaxation with a broad relaxation time distribution, the Cole-Cole single relaxation time formula should be modified. In figure 4(b), the solid line is the fitting of the data with a modified Cole-Cole equation,

$$\varepsilon^*(\omega) = \varepsilon_u + \frac{\varepsilon_R - \varepsilon_u}{1 + (i\,\omega\,\tau_0)^\beta} \qquad (5)$$

which describes the dielectric dispersion with a broad distribution of the relaxation time centered at τ_0 where ω is the angular frequency. In eq. (5), $0 < \beta \leq 1$ measures the width of the relaxation time distribution and when $\beta = 1$, eq. (5) is reduced to the single relaxation time Cole-Cole equation and a smaller β corresponds to a broader distribution of the relaxation time. For the data in figure 4(b), the fitting yields $\beta = 0.22$ indicating the existence of a broad distribution of the relaxation in the material and the τ_0 at 0 °C is $2.2*10^{-4}$ seconds.

In addition, it was found that the shifting factor a(t) follows the WLF relation[10]

$$a(t) = -\frac{c_1(t - t_g)}{c_2 + t - t_g} \qquad (6)$$

with $c_1 = 21.1$, $c_2 = 54.1$, $t_g = 220.0$ K. The glass transition temperature t_g at 220 K (= - 53.15 °C) is consistent with the data presented in figure 3. It should be pointed out that the parameters c_1 and c_2 obtained here are close to the universal constants c_1^g and c_2^g which have approximate values of 17.44 and 51.6 respectively.[10] At temperatures above 40 °C, there is a relaxation peak (I-relaxation) in addition to the α-relaxation as shown in figure 4(c). The temperature shifting factors for the two relaxations are different as they should be. Due to this fact, no attempt was made to generate a master dispersion curve in that temperature range. A detailed data analysis indicates that the I-relaxation also follows the WLF relation and in the temperature region where both the I-relaxation and β-relaxation exist, there is a coupling between the two relaxations, which will be discussed in another publication.

The elastic compliance measured at temperatures about the glass transition is presented in figure 5. Apparently, there is more than one order of magnitude change in the elastic compliance of the material as it goes through the glass transition. Using the temperature-frequency superposition principle, the elastic compliance curve at 0 ^{o}C over a frequency range from about 10^{-2} Hz to above 10^{3} Hz can be obtained as shown in figure 6(a). The elastic compliance changes by more than one order of magnitude in this frequency range. The shifting factor for the elastic compliance also fits well with the WLF relation as shown in figure 6(b) yielding c_1 = 19.9, c_2 = 125.4, and a glass transition temperature t_g = 252.3 K. The higher glass transition temperature obtained from the elastic compliance data compared with that from the dielectric constant indicates that in the polyurethane elastomer investigated, for the α-relaxation (the glass transition), the average energy barrier for the chain segment motions related to the strain and stress is higher than that for the motions not strain and stress related (pure dielectric). We will come back to this point later in the paper.

The data in figure 6(a) was also fitted with the relaxation equation (5) where the dielectric constant is replaced by the elastic compliance. The solid curve in figure 6(a) is the result of the fitting and apparently, the data can be described quite well by eq. (5) which yields β = 0.32 and $\tau_0 = 6 * 10^{-2}$ seconds. Compared with the parameters from figure 4(b) of the dielectric data (at the same temperature), the relaxation distribution of the elastic process in the material is narrower (a larger β) and the average relaxation time τ_0 is longer, which is consistent with the results presented in the preceding paragraph that the energy barriers for the segment motions which generating strain are higher than those of non-strain related segment motions. From the fact that both eq. (5) and WLF relation describe the mechanical relaxation data rather well, we tried to combine eq. (5) with the WLF relation

$$\log \tau_0 = \log \tau_g - \frac{c_1(t - t_g)}{c_2 + t - t_g}$$

to fit the data in figure 5. Indeed, the data in figure 5 can be described well as demonstrated by the solid curve in the figure for the data at 30 Hz. The fitting yields $\beta = 0.34$, $c_1 = 16.5$, $c_2 = 144$, and a glass transition temperature $t_g = 255$ K. Evidently, the results of the fitting to the two sets of data are quite consistent with each other, especially the value of the glass transition temperature.

It has been shown that the electric field induced strain in the polyurethane samples is proportional to the square of the applied electric field. Hence, a parameter R_{33} is introduced to describe the sensitivity of the strain response of the material to an applied electric field

$$S_3 = R_{33} E^2.$$

Presented in figure 7 is R_{33} as a function of frequency characterized in the temperature range from - 30 °C to 80 °C. R_{33} is always less than zero indicating that an applied electric field causes a contraction in the specimen in the direction parallel to the applied field. In analogy to the dielectric constant and elastic compliance, R_{33} also exhibits a strong frequency dependence. Making use of the dielectric constant and the elastic compliance data, the contribution of Maxwell stress to the total strain response in the material can be evaluated, which is shown in figure 8(a) along with the total strain response at 10 Hz and 100 Hz where the Maxwell stress term is $R_m = -s_{33} \varepsilon_0 K / 2$. Evidently, at temperatures above 20 °C, the contribution from Maxwell stress is significant. On the other hand, the non-Maxwell stress part or the contribution related to the true electrostriction, which is the difference in figure 8(a) between R_{33} and R_m, is also quite sizable. Based on eq. (2), the electrostrictive coefficient for the material as a function of frequency and temperature is evaluated and presented in figures 8(b) and 8(c). Unlike the ferroelectric ceramic materials where Q is nearly independent of temperature and frequency, the electrostrictive coefficient for the polyurethane elastomer depends on frequency markedly and weakly on temperature in the temperature range investigated. The relatively large data scatter in figures 8(b) and 8(c) is caused by the fact that the data are obtained from three sets of data, i.e., R_{33}, K, and s_{33}, each of which contains data scatter. The decrease of the Q with frequency indicates that the

component of the polarization motions of high frequency (short relaxation times) does not generate strain in the material and hence are pure dielectric, which is consistent with the results from the dielectric and elastic complaince data that the energy barrier for the segment motions which generate strain response is higher than that of non-strain related segment motions.

In Table I, the electrostrictive coefficients Q_{11} from several commonly used ferroelectric materials are compared with that of polyurethane elastomer investigated. The Q for the polyurethane elastomer investigated is much larger than those of the other materials. Although the detailed mechanisms of the electrostriction in a material depends on the molecular bases generating it such as the ionic displacement and polarization orientation effect on which very little understanding exists, there exist empirical relationships which seem to be consistent with the

Table I. Comparison of the electrostriction coefficients and related properties

Materials	Q_{11} (m^4/C^2)	K	s (10^{-11} m^2/N)
PMN-PT[15,16]	0.02	25,000	1.0
PZT[17]	0.096	2,000	1.6
PVDF[6,18]	- 2.0	9	30
Polyurethane	- 150 -- 450	4 -- 8	$5 * 10^2$ -- $5 * 10^3$

a. Q_{11} is the longitudinal electrostrictive coefficient, K is the dielectric constant, and s is the elastic compliance.

experimental results on the electrostrictions from different materials. For instance, it has been observed that the electrostrictive coefficient Q is inversely proportional to the dielectric constant and proportional to the elastic compliance of the material.[14] As shown in Table I, these rules can

qualitatively describe the data for PMN, PZT and PVDF. However, for the polyurethane elastomer, in the temperature range from -30 C to 20 C, the elastic compliance reduces more than one order of magnitude (figure 5) while the change of Q in the same temperature range (figure 8(c)) is relatively minor, which seems not consistent with the empirical rule between Q and compliance of the material.

In order to provide understanding on these findings, it is instructive to consider general features of electrostrictive coefficient for a material with a broad relaxation time distribution as in the polyurethane elastometers here. As we have pointed out, when dealing with the electromechanical response in a polymeric material, one has to distinguish between the polarization motions associated with the strain and stress and the ones not associated with them. The later ones can be envisioned as a pure 180° flipping of a dipole, which can be either a single chain segment motion or a result of a collective motion of several molecular units and chain segments. There are different relaxation time distributions for these two types of components as schematically drawn in figure 9(a). For the polyurethane elastomers investigated, it seems to be that the high frequency components of the polarization motions do not contribute to the strain response as much as the low frequency components yielding a decrease of Q with frequency. Using the scenario that the relaxation time of the dipole orientation is related to the energy barrier for that motion, the results imply that the energy barriers for the polarization change which generates strain response are higher that those for non-strain related polarization changes. Therefore, how Q changes with frequency will depend on how the ratio between the polarizations which is strain related and those of non-strain related varies with temperature and frequency. In general, there is no reason that such a process will simply follow the temperature frequency superposition principle.

With regards to the relationship between the elastic compliance and the electrostrictive coefficient, it is also instructive to consider two different groups of the chain segment and molecular unit motions in an elastic process, i.e., the ones of pure elastic and the ones related to

the polarization changes. To aid this analysis, a general scenario of the chain segment motions in a polymeric material is drawn schematically in figure 9(b), where we divide the motions of polymer chain segments and molecular units into the ones associated with the polarization process (contributing to the dielectric response and assigned as the type I motion) and the ones associated with the elastic process (contributing to the elastic compliance and assigned as the type II motion). Apparently, the ones which are in the overlapping zero of the two contribute to the electromechanical response of the material. Therefore, there is no direct relationship between the electrostrictive coefficient Q and the elastic compliance of a material. On the other hand, if a material has a large compliance, which implies that the energy barriers for the mechanical related segment motion is relatively low, it will increase the ratio between the overlap region and the type I region and result in a higher electrostrictive coefficient.

Both the higher freezing temperature for the polymer chain segment motions associated with the mechanical response (elastic compliance) of the polyurethane and the decrease of the electrostrictive coefficient with frequency indicate that in the temperature range investigated the energy barriers for these motions are higher than the ones not associated the mechanical response. The investigation on the molecular origin of this phenomenon is currently underway.

IV. FTIR and DSC Results of the Phase Transitional Phenomena

To understand how the observed macroscopic properties are related to the morphology and molecular structure, differential scanning calorimetry (DSC) and Fourier transform infrared (FTIR) spectroscopies of the polyurethane were examined as a function of temperature. The temperature range for both DSC and FTIR measurements was from 25 °C to 180 °C.

The results obtained from these analysis indicate the observed changes in the electrostrictive, dielectric and elastic properties at the temperatures of around 70 °C might be attributed to the relaxation of the extender in the hard segments. DSC curve, which is shown in figure 10, shows an endothermic peak around 70 °C, starting at around 50 °C and ending at

around 85 °C, which is much higher than the glass transition temperature (about -20 °C), and obviously lower than the melting temperature, which is about 170 °C. Since the glass transition reflects the change in the molecular motions of the soft segments and the melting is related to the transition of the molecular flow of the polymer chains, the peak in between may be related to the molecular relaxation associated within the hard segments, most possibly, the extenders, since the dissolution of the MDI will cause the melting. FTIR spectroscopy data on the temperature dependence of the hydrogen bonding in the polyurethane, which are shown in figures 11a-11d, support this hypothesis. As the temperature is increased, the absorbance of bonded -NH (3327 cm^{-1}) associated with the absorbance of -C=O (1714 cm^{-1}) decrease while the absorbance of unbonded, or free, -NH (3448 cm^{-1}) and the unbonded -C=O (1730 cm^{-1}) increase. The relatively large change can be observed between 60 °C and 140 °C, which coincides with the second endothermic peak observed in DSC measurement. The consistence of the results obtained in DSC and FTIR indicates that the anomalous changes observed in the macroscopic properties at temperatures around 70 °C can be attributed to the molecular motion of extenders in the hard segments. The higher transition temperature observed in the FTIR study than that from the DSC analysis might be the result of the restraining of the MDI, which holds the separation of -NH from -C=O not going to far until temperature is high enough to cause MDI molecular motion to be significant.

V. ESCA and Neutron Surface Reflectivity Experiments on the Possible Non-uniform Distribution of the Hard Segments and Soft Segments across the Sample Thickness Direction

Inhomogeneity in a multi-component material is a factor which should be considered since it may cause non-uniform distribution of internal electric field, which will affect the electrostrictive response. For the polyurethane elastomer investigated, there are two components in the material, i.e., the hard segments and soft segments. Knowing the distribution of the two segments in the polyurethane films should be helpful to understand mechanisms of the electric

induced strain in the material. Electron Spectroscopy for Chemical Analysis (ESCA) and Small Angle Neutron Reflectivity were carried out toinvestigate the distribution profile of the two segments along the thickness direction.

The results of the ESCA analysis on the surface composition of the polyurethane film is tabulated in the table below

Peak	Position-(BE/eV)	FWHM-(/eV)	Raw area	Atomic mass	Atomic-conc. %
C 1s	288.40	1.58	288039	12.00	92.51
O 1s	536.00	2.39	59027	16.00	7.18
N 1s	403.60	1.84	1639	14.00	0.31

As can be seen, the atomic concentration of nitrogen (N 1s) in the surface is 0.31%, which is significant lower than the calculated atomic concentration of N 1s in a homogeneous bulk sample (about 1.5%). Since only the hard segments contain N-atom, the fewer N-atom in the surface region indicates there are fewer hard segments in the free surface region. Therefore, the result qualitatively confirms that the distribution of the two segments is not homogeneous along the thickness direction.

To study the distribution profile of the two components along the thickness direction, the Neutron Reflectivity technique was employed. Since the neutron scattering cross sections of the hard segment and the soft segment are different, the neutron reflectivity pattern is expected to reflect this if the ratio of the two changes along the thickness direction, or a distribution profile exists. The samples for the experiment was prepared by casting the films on the silicone wafer. In the experiment, it was found that the signal of the reflectivity from samples was weak. The reason for the weak signal might be the quality of the sample surface (roughness). Since the enhanced field induced strain response was observed even in a relatively thick film (0.2 mm) which indicates the depth of the non-uniform profile can be quite deep, a thicker film is required to mimic the true experimental condition. However, in the spin coated film, as the thickness of

the film increases, the roughness of the sample surface also increase proportionally so the surface quality of the sample becomes worse. The results of the neutron reflectivity experiment is shown in figure 12. As can be seen, it seems that reflectivity profile shows oscillations at the higher Q range which implies the existence of a surface profile related to the change in the ratio between the two segments. The weak signals do not allow us to make a quantitative data analysis, especially, at the low Q range where the effect of the surface roughness on the data is more severe. To improve the results of neutron reflectivity experiment, a new sample preparation method will be developed to improve the surface quality of the sample. Meanwhile, we are also considering to enhance the reflectivity contrast by deuterizing one of the components.

VI. The Hydrostatic Pressure Depandence of the Dielectric Constant and the Converse Electrostrictive Effect in Determining the Electrostrictive Coefficient

The pressure dependence of the dielectric constant of the polyurethane elastomer was determined in the pressure range from 0 to 20,000 psi and temperatures from 0 °C to 80 °C. The data are presented in figure 13 which were acquired at 0 °C, 29 °C, 50 °C, and 80 °C. Apparently, the dielectric constant exhibits relatively large change with the hydrostatic pressure. It is well known that through the converse electrostrictive effect, the electrostrictive coefficient of a material can be determined from the change of the dielectric constant with stress (or pressure).

From the equilibrium thermodynamics, it can be shown that the electrostrictive coefficient can also be determined by the so-called converse electrostrictive effect, i.e., the change of the equilibrium dielectric constant with stress. Utilizing the Maxwell relation, one can derive:

$$\frac{\partial K}{K \partial p} = -2 \varepsilon_0 K Q_h \qquad (7)$$

where p is the hydrostatic pressure and Q_h is the hydrostatic electrostrictive coefficient of the material. Although eq. (7) has been widely used in early studies, it is a common mistake that many people ignored the fact that eq. (7) is derived under thermodynamic equilibrium condition, that is, it cannot be used to describe the frequency dependence behavior of Q_h. For a material

possessing a strong relaxation such as the polyurethane elastomer investigated, its frequency diepersion can be described by eq. (5) and eq. (7) is valid in describing the pressure dependence of ε_R, not $\varepsilon(\omega)$. As the material is subjected to a hydrostatic pressure, the change of the dielectric constant is caused by two factors, one is the shift of the relaxation time τ_0 and the other is the change of $\varepsilon_R - \varepsilon_u$ with pressure. The shift of the relaxation time is not directly related to the electrostrictive coefficient. In order to deterimne how ε_R changes with pressure, eq. (5) should be used to fit the data in figure (ε_u usually does not depend on the pressure). From the fittiing, the variation of ε_R with pressure can be obtained and hence, the electrostrictive coefficient Q_h. The data analysis is currently underway and the result will be reported in the near future.

VII. A New Apparatus for the Field Strain Measurement of Thin and Soft Polymer Samples

The intention is to use the sensor from a phonograph cartridge as a displacement measuring device which may have the advantages of easy to use and that it can be used to measure the field induced strain on soft and thin polymeric materials reliably. Phonograph records encode sound in terms of displacements in two orthogonal directions in the helical surface tracks of vinyl disks. The demands of audiophiles have been forcing the commercial development of phonograph cartridges since not long after their invention by Thomas Edison. Consequently, phonograph cartridges are well-developed, low noise, highly sensitive transducers which require only a few grams of contact force and operate over the entire audio range.

The first attempt at using a phonograph cartridge involved a modern magnetic pickup type cartridge. Basically a small permanent magnet is moved by the motion of the needle in a small coil. The voltage output of such a system is proportional to the velocity of the magnet and is typically quoted as 5 mV at 5 cm/s (when measured at 1 kHz). Because the output is proportional the velocity this cartridge proved unsatisfactory at frequencies below 1 kHz.

A second attempt used a much older technology. Before moving magnet and moving coil cartridges were common, phonographs cartridges used a small piezoelectric bimorph as a displacement sensor. The bimorphs were typically 15 mm long, 3 mm across, and 1 mm thick. The motion of the needle stresses the bimorph and produces an output charge or voltage propriate to our needs. It has flat frequency response, even into the sub-audio range, and has a higher signal-to-noise ratio than the moving magnet, at least below 1 kHz, Although there is some variation in output from bimorph to bimorph and from each construction, the output is typically 10-2 c/m. Under realistic conditions this means that a resolution of one picometer is available. The biggest single problem is electrical pickup from the signal driving the sample which can couple directly into the bimorph output and produce spurious signal. This effect can be effectively eliminated with careful attention to electrical shielding. Figure 14 shows a diagram of the displacement sensor constructed from the piezoelectric bimorph removed from a ceramic phonograph cartridge. For the sake of clarity, no electrical shielding is shown.

References:

1. W. G. Cady, "Piezoelectricity" (Dover Publications, Inc., New York 1964).

2. J. M. Herbert, "Ferroelectric Transducers and Sensors" (Gordon and Breach Science Publishes, N. Y. 1982).

3. B. Jaffe, W. R. Cook, Jr., and H. Jaffe, "Piezoelectric Ceramics" (Academic Press, London and N. Y. 1971).

4. A. J. Lovinger, Science 220, 1115-1121 (1983).

5. H. R. Gallantree, IEE Proceedings 130, 219-224 (1983).

6. H. Wang, Ph. D. Thesis, The Pennsylvania State University (1994).

7. M. Zhenyi, J. I. Scheinbeim, J. W. Lee, and B. A. Newman, J. Polym. Sci. Part B: Polym. Phys. 32, 2721 (1994).

8. H. Wang, Q. M. Zhang, L. E. Cross, R. Ting, C. Coughlin, and K. Rittenmyer, Proc. Int. Symp. Appl. Ferro. 9, 182 (1994).

9. I. Ladabaum, B. T. Khuri-Yakub, D. Spoliansky, Appl. Phys. Lett. 68, 7 (1996).

10. N. G. McCrum, B. E. Read, and G. Williams, "Anelastic and Dielectric Effects in Polymeric Solids" (Dover Publications, Inc. New York 1967).

11. P. Wright and A. P. C. Cumming, "Solid Polyurethane Elastomers" (Gordon and Breach Sci. Pub., N. Y. 1969).

12. Q. M. Zhang, S. J. Jang, and L. E. Cross, J. Appl. Phys. 65, 2807 (1989).

13. Y. Tada, Jpn. J. Appl. Phys. 34, 1595 (1995).

14. V. Sundar and R. E. Newnham, Ferro. 135, 431 (1992).

15. J. Zhao, Q. M. Zhang, N. Kim, and T. Shrout, Jpn. J. Appl. Phys. 34, 5658 (1995).

16. E. A. McLaughlin, J. Powers, M. B. Moffett, and R. S. Janus, data presented at 1996 ONR Review on Transducer and Transducer Materials, The Pennsylvania State University (1996).

17. M. Haun, Ph. D. Thesis, The Pennsylvania State University (1983).

18. T. Furukawa and N. Seo, Jpn. J. Appl. Phys. 29, 675 (1990).

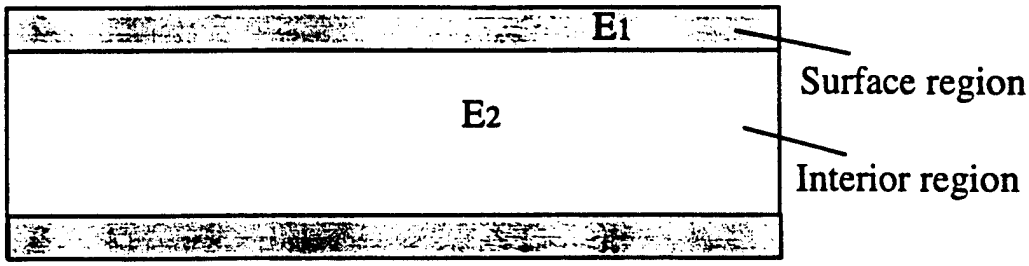

(a)

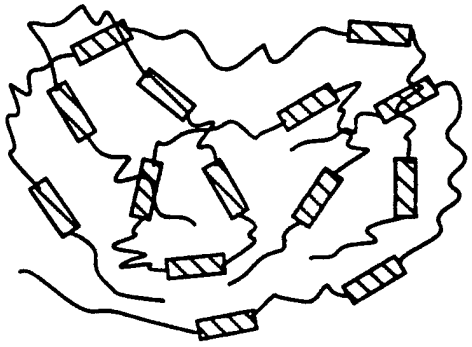

(b)

Figure 1. (a) Schematical drawing of a polyurethane sample showing the surface region (hatched regions) and interior region. The electric fields in the two regions E_1 and E_2 may be different. The existence of the two regions causes the thickness dependence of the electric field induced strain response. (b) Schematical drawing of the morphology of a polyurethane elastomer where the hard segments (hatched boxes) are embedded in the matrix of soft segments (thin lines).

Fig. 1

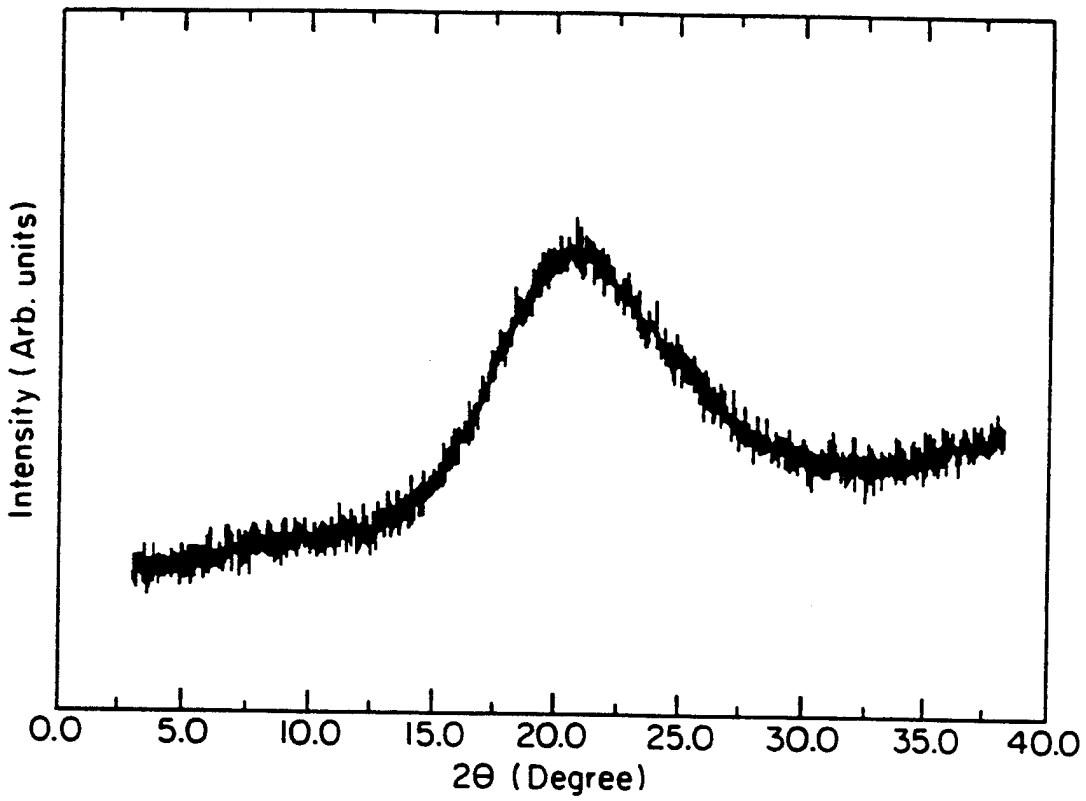

Figure 2. X-ray diffraction data of the polyurethane elastomer at room temperature where the broad near 20° is the amorphous hola. No crystalline phase can be detected within the data resolution.

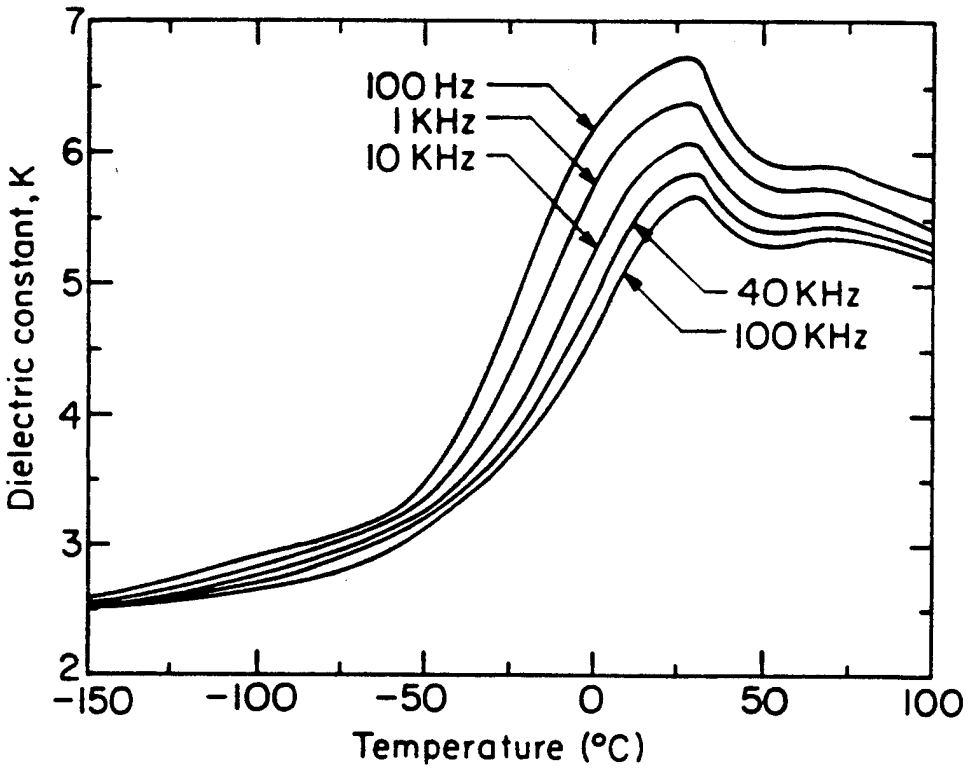

Figure 3. Weak signal dielectric constant as a function of temperature for the polyurethane elastomer where the measuring frequencies are 0.1, 1, 10, 100 kHz.

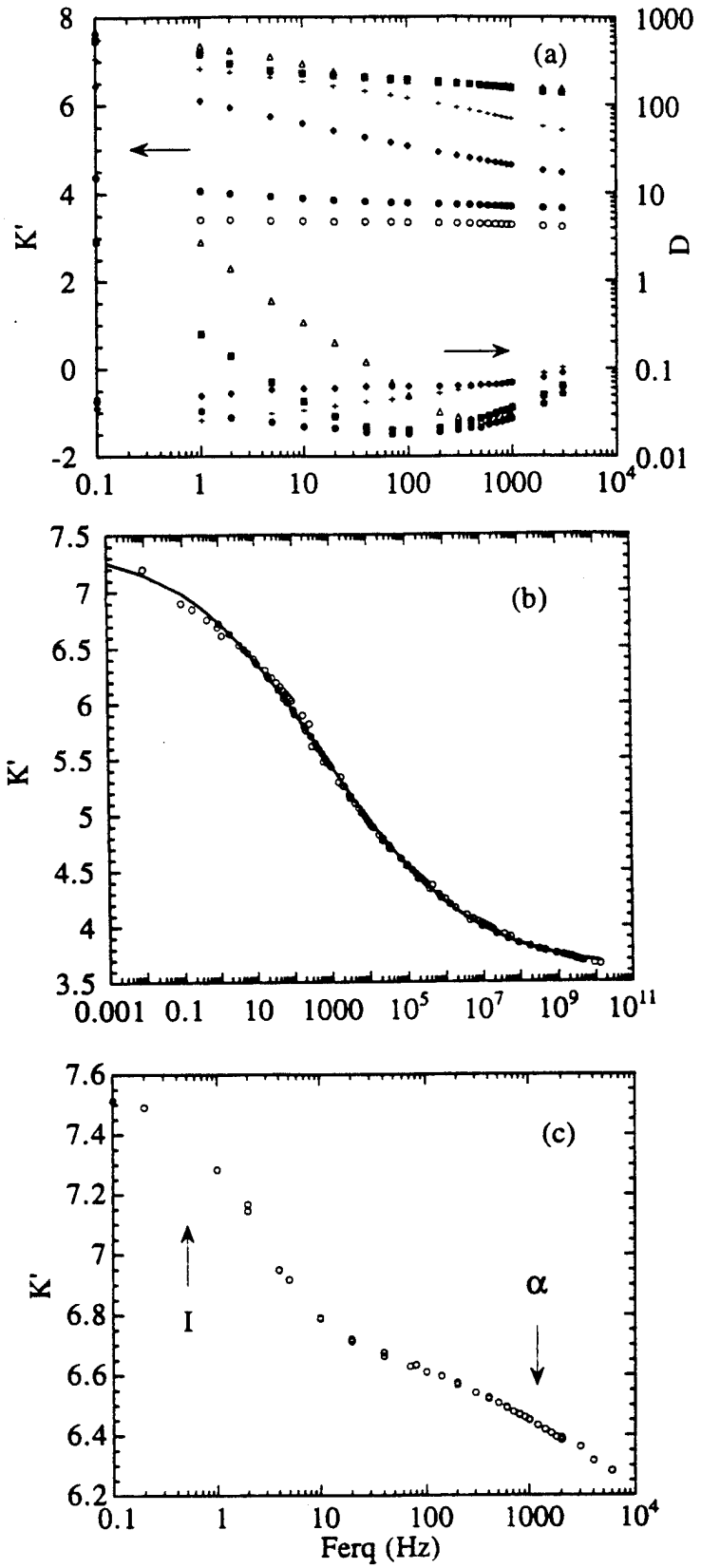

Figure 4. (a) Weak field dielectric constant as a function of frequency for temperatures 80 °C (open triangles), 50 °C (solid squares), 5 °C (plus signs), -15 °C (solid diamonds), -40 °C (solid circles), and -80 °C (open circles). (b) Master curve of the dielectric constant at 0 °C where open circles are the data point and solid line is from the fitting using eq. (5). (c) Dielectric constant at 60 °C which shows clearly two relaxation processes (labeled as I and α).

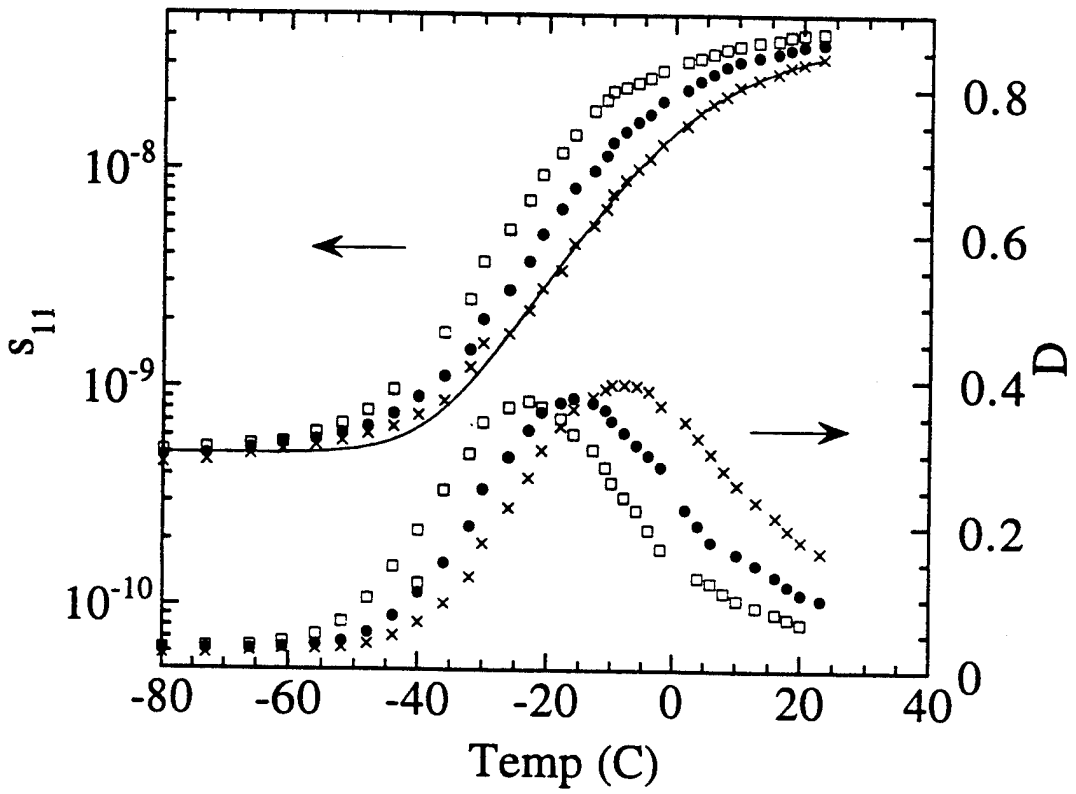

Figure 5. The elastic compliance in the temperature range about the glass transition. The measuring frequencies are 0.3 Hz (open squares), 3 Hz (solid circles), and 30 Hz (crosses). The solid line at 30 Hz data is the fitting result.

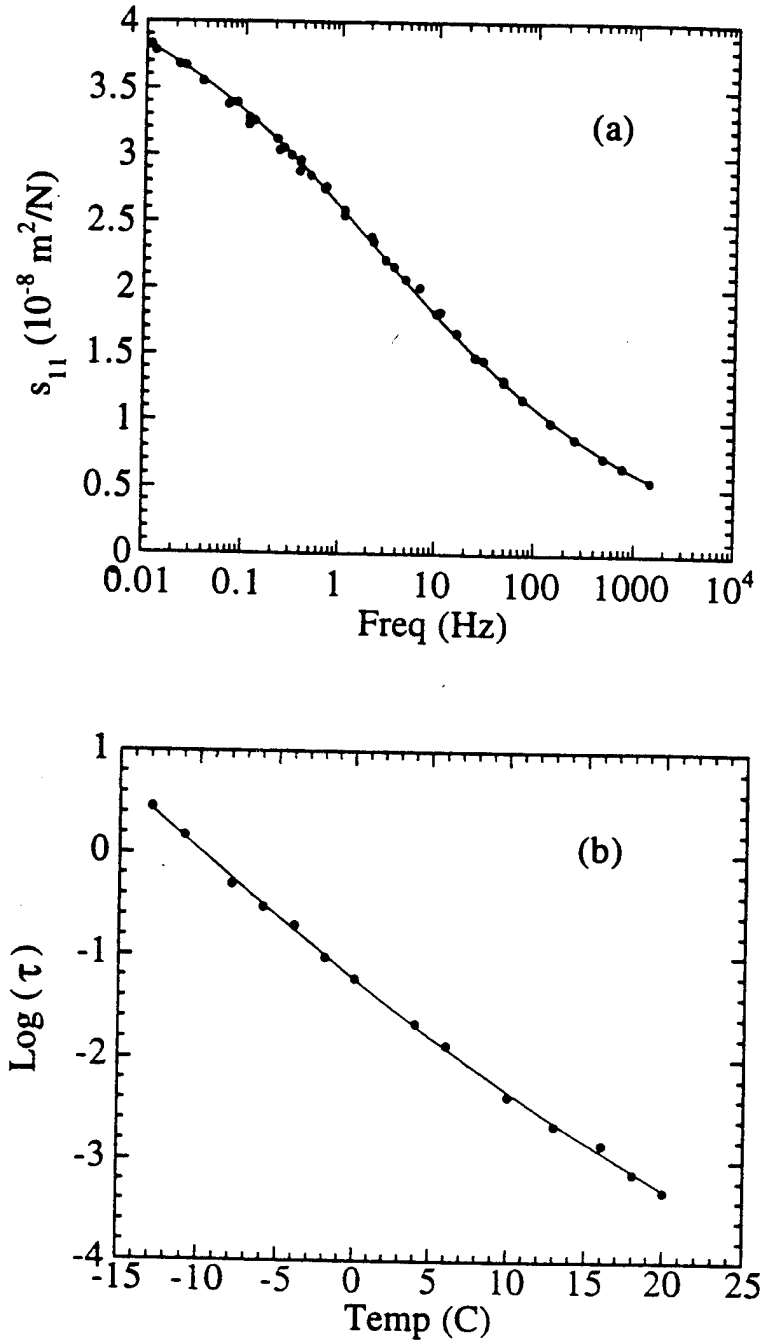

Figure 6. (a) The master curve for the elastic compliance at 0 °C where the solid line is from the fitting. (b) The change of the relaxation time with temperature from the elastic compliance data where solid circles are the data and solid line is the fitting using WLF relation.

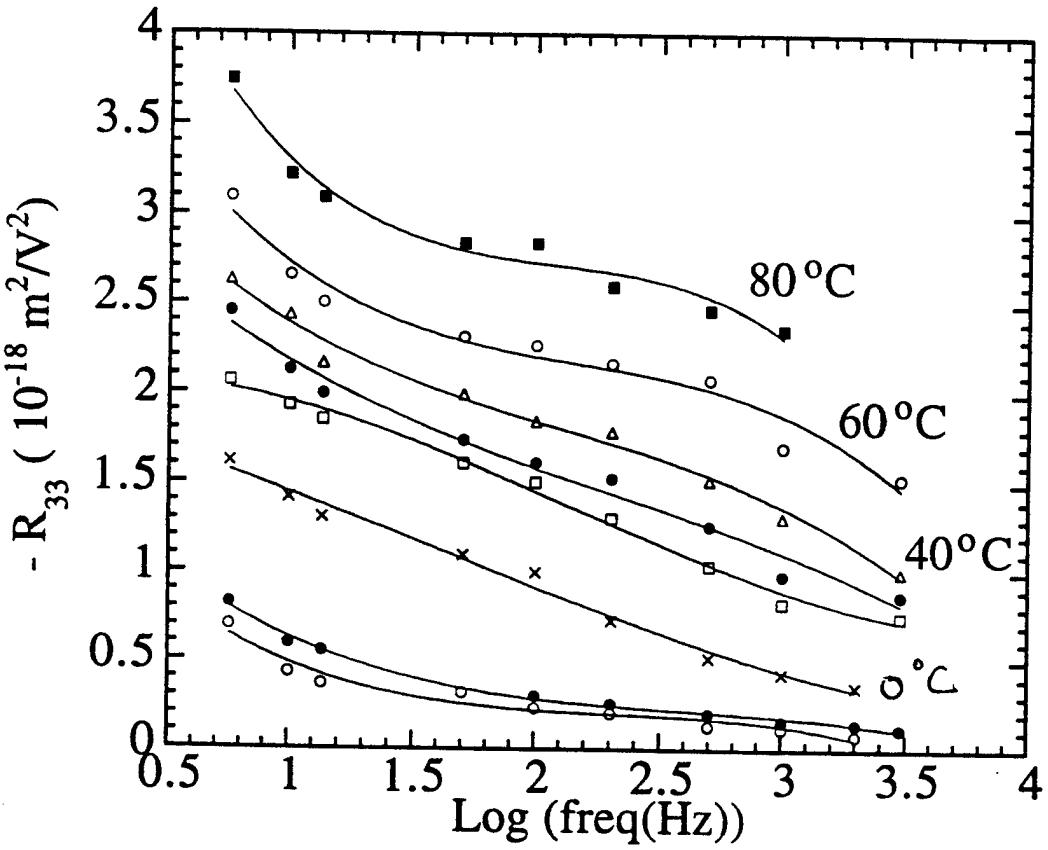

Figure 7. R_{33} as a function of frequency at different temperatures (from top to bottom): 80 °C solid squares), 60 °C (open circles), 40 °C (open triangles), 30 °C (solid circles), 20 °C (open squares), 0 °C (crosses), -20 °C (solid circles), and -28.3 °C (open circles). The solid lines are drawn to guide eyes.

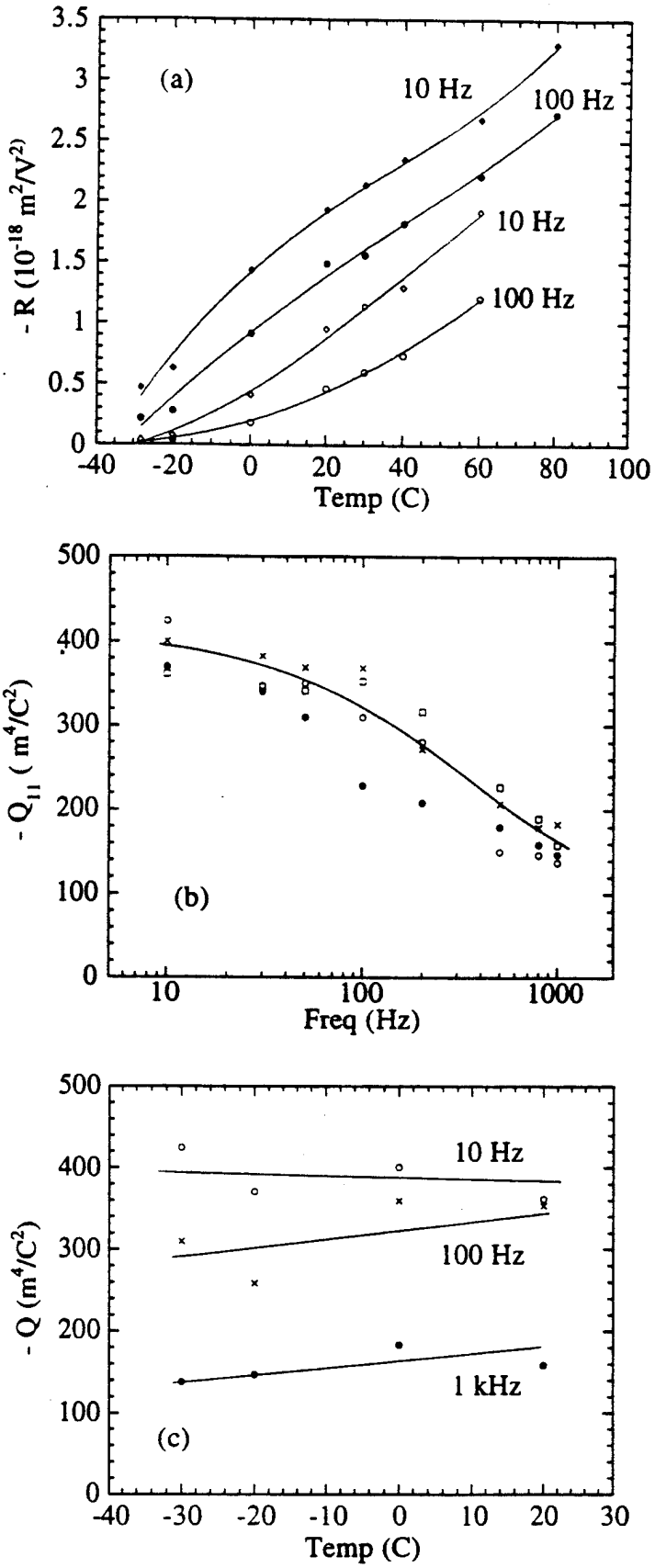

Figure 8. (a) Comparison between R_{33} (solid diamonds and circles) and the contribution from the Maxwell stress effect R_m (open diamonds and circles) at 10 Hz and 100 Hz. The solid lines are drawn to guide eyes. (b) The electrostrictive coefficient as a function of frequency at temperatures of -30 °C (open circles), -20 °C (solid circles), 0 °C (crosses), and 20 °C (open squares). (c) The electrostrictive coefficient as a function of temperature in the temperature range from -30 °C to 20 °C at different frequencies: 10 Hz (open circles), 100 Hz (crosses), and 1 kHz (solid circles).

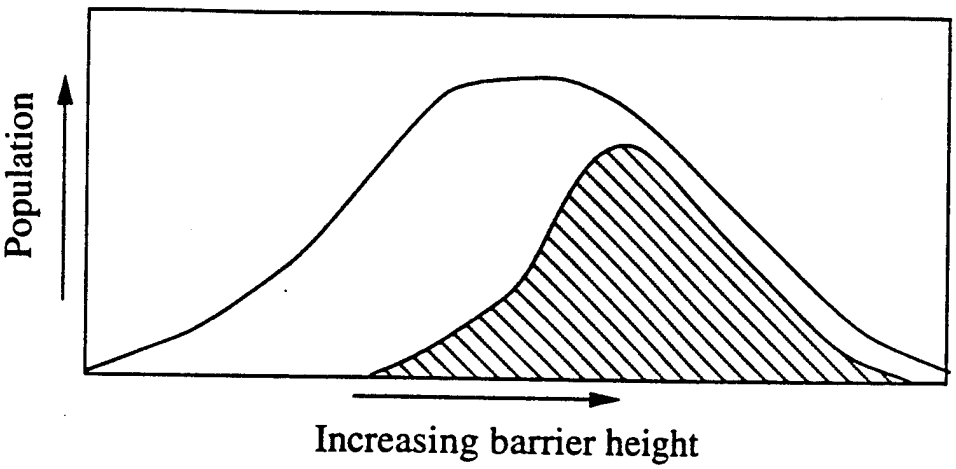

(a)

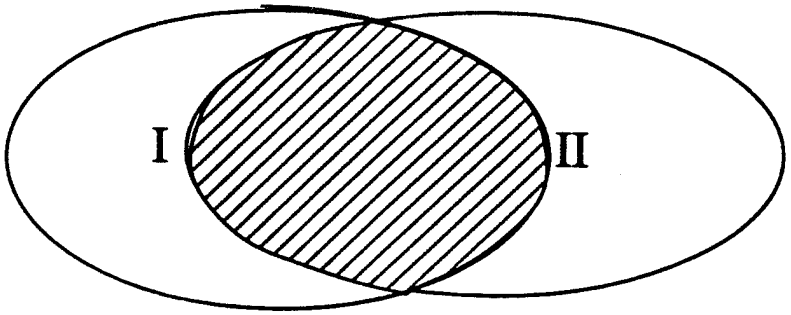

(b)

Figure 9. (a) Schematical drawing showing the different energy barrier distributions in the dielectric response for the chain segment motions associated with the strain and stress (hatched region) and the segment motions which do not produce strain response (dotted region) in a polymer sample. (b) Schematical drawing which divides the polymer chain motions into those related to the dielectric response (type I) and those related to the mechanical response (type II). The part of the chain segment motions contributing to both the dielectric and mechanical responses is the region which is the overlap between the type I and type II region (hatched region).

F.9.

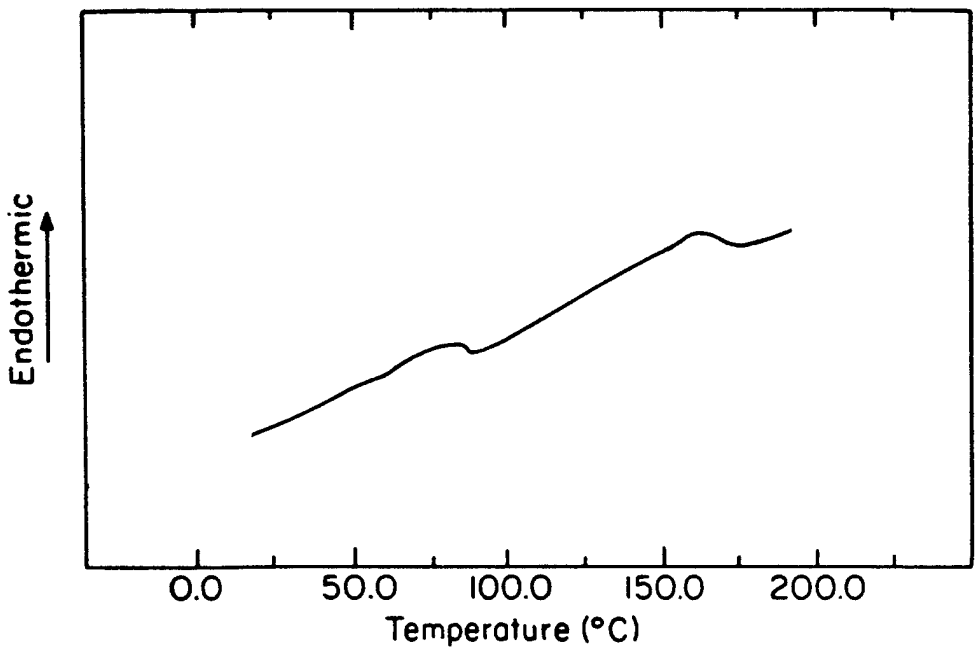

DSC curve of the polyurethane elastomer 2105-80AE sample.

Fig. 10

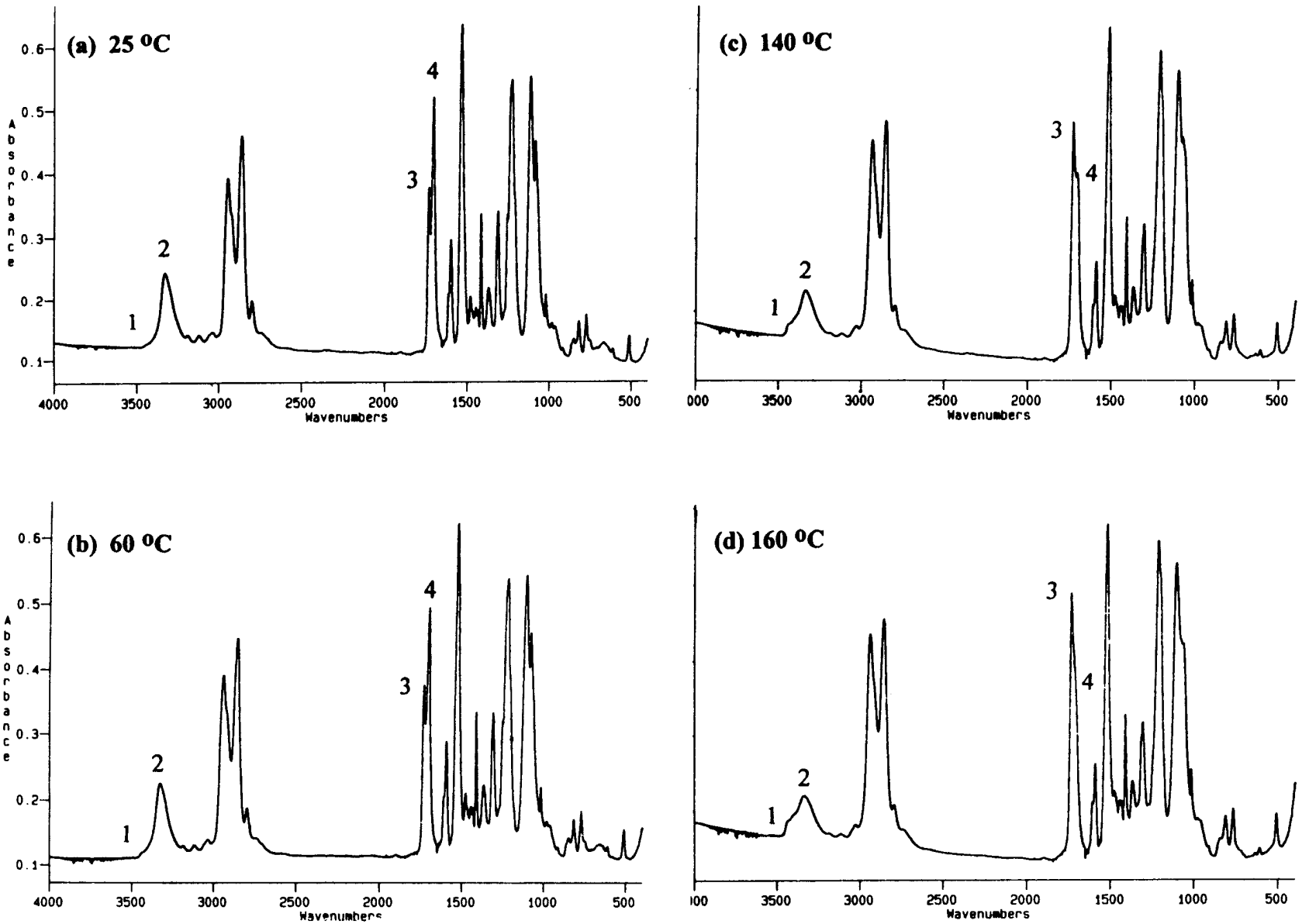

FTIR spectroscopy of polyurethane elastomer 2105-80AE at the temperature of 25 °C, 60 °C, 140 °C and 160 °C. (1: 3448 cm^{-1} 2: 3327 cm^{-1} 3: 1730 cm^{-1} 4: 1714 cm^{-1})

Fig. 11

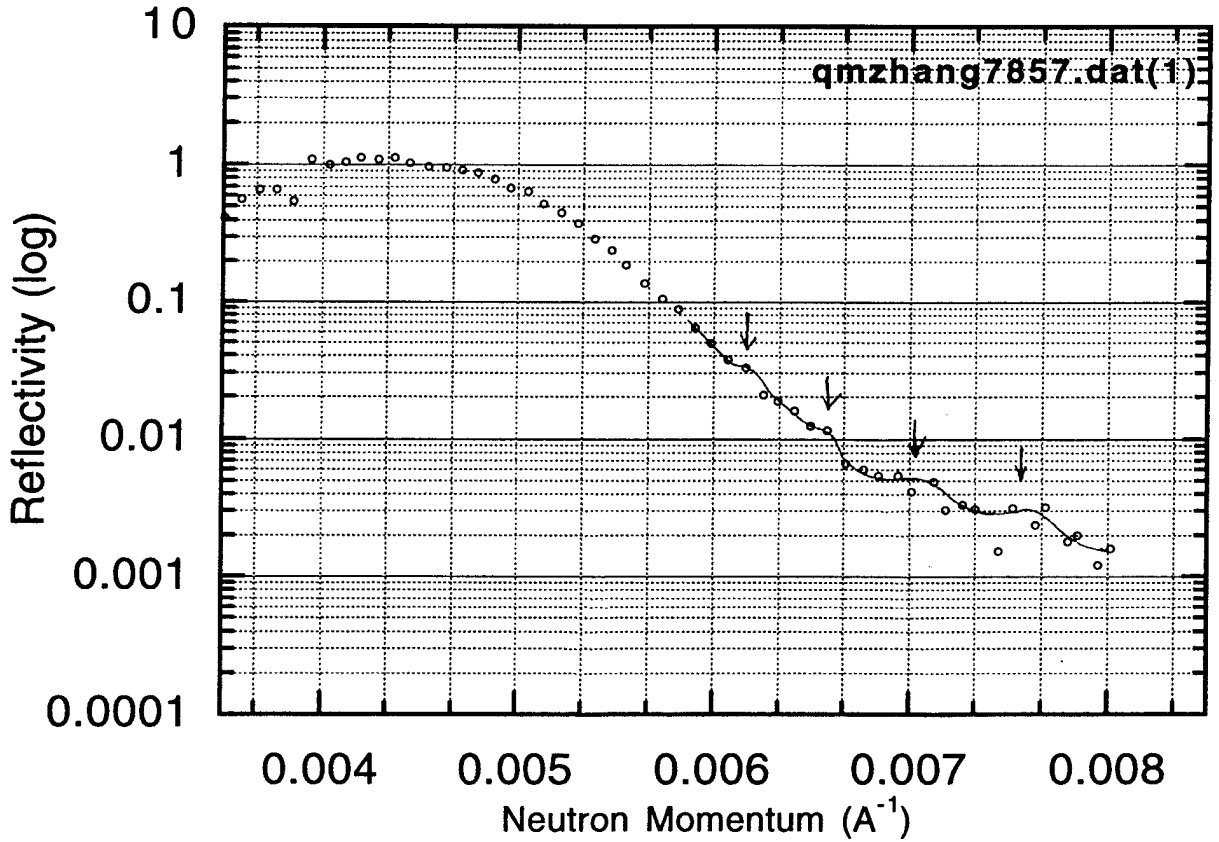
qmzhang7857.dat(1)
10
1
0.1
0.01
0.001
0.0001
Reflectivity (log)
0.004
0.005
0.006
0.007
0.008
Neutron Momentum (A-1)

Fig. 12

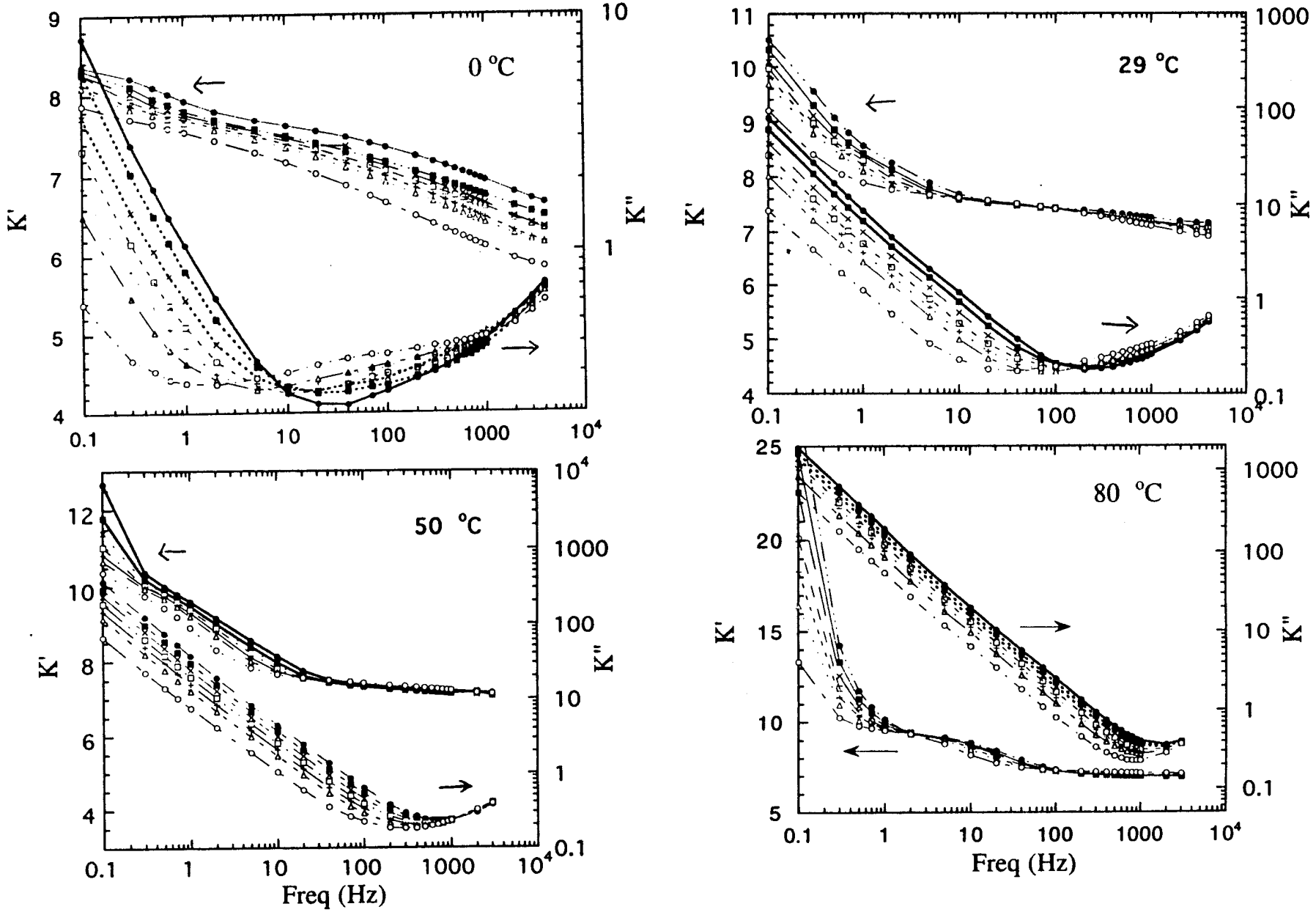

Figure 13. The hydrostatic pressure dependence of the dielectric constant of the polyurethane elastomer at different temperatures (0 °C, 29 °C, 50 °C, and 80 °C). The hydrostatic pressure: 0 psi (solid circles), 2,500 psi (solid squares), 5,000 psi (crosses), 7,500 psi (open squares), 10,000 psi (plus sign), 12,500 psi (open triangles), and 20,000 psi (open circles).

Fig. 1

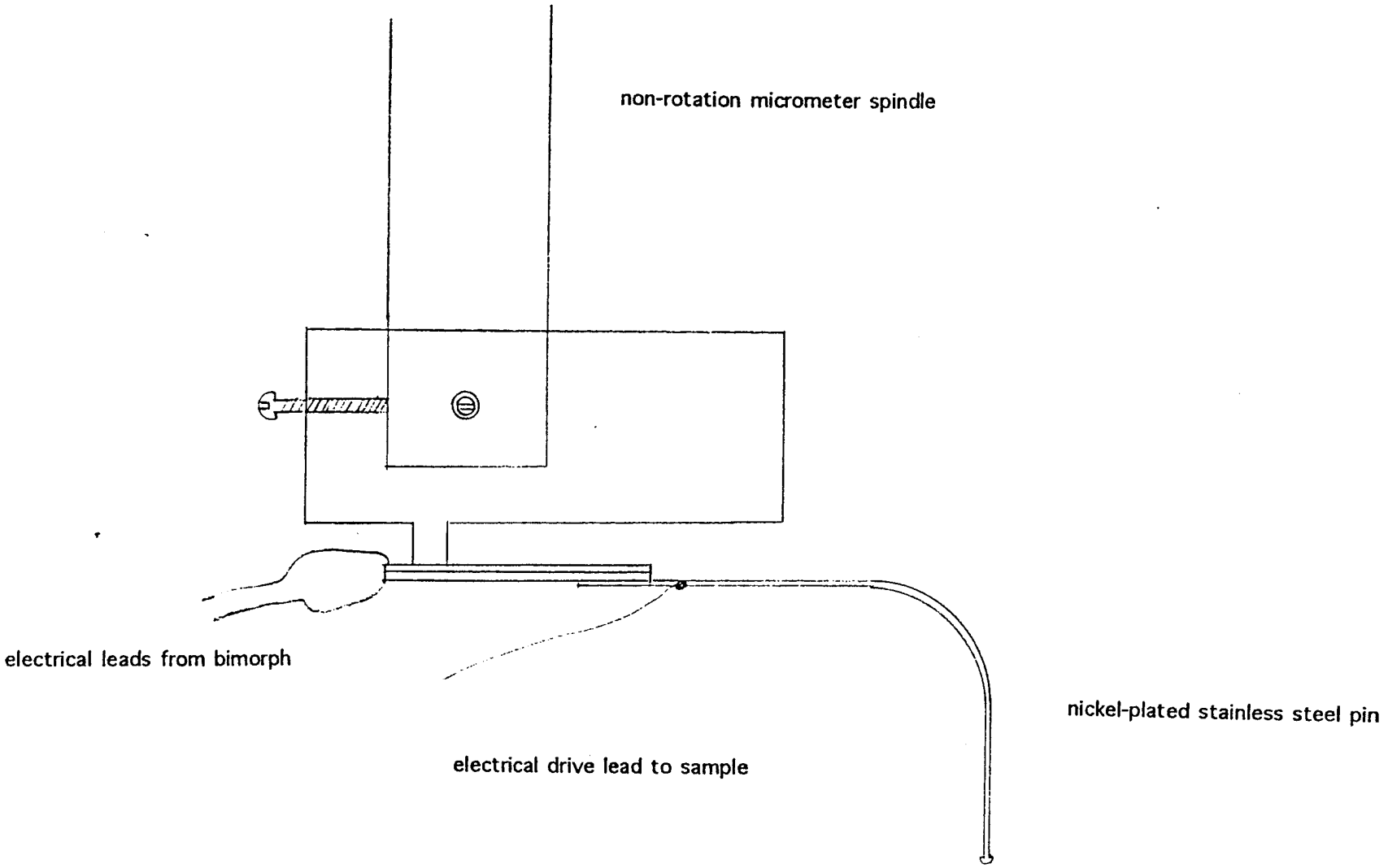

Figure 14. Schematic drawing of the new set-up which is currently under test for the field induced strain measurement on thin and soft polymeric samples.

Fig. 14